NASA TN D-449

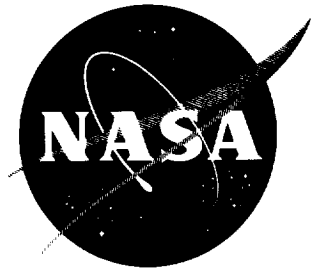

TECHNICAL NOTE

D-449

INVESTIGATION OF THE FLOW OVER SIMPLE BODIES AT MACH NUMBERS OF THE ORDER OF 20

By Arthur Henderson, Jr.

Langley Research Center
Langley Field, Va.

NATIONAL AERONAUTICS AND SPACE ADMINISTRATION

WASHINGTON

August 1960

1V

NATIONAL AERONAUTICS AND SPACE ADMINISTRATION

TECHNICAL NOTE D-449

INVESTIGATION OF THE FLOW OVER SIMPLE BODIES AT MACH NUMBERS OF THE ORDER OF 20

By Arthur Henderson, Jr.

L
1
0
5
1

SUMMARY

It is shown that adequate means are available for calculating inviscid direct and induced pressures on simple axisymmetric bodies at zero angle of attack. The extent to which viscous effects can alter these predictions is indicated.

It is also shown that inviscid induced pressures can significantly affect the stability of blunt, two-dimensional flat wings at low angles of attack. However, at high angles of attack, the inviscid induced pressure effects are negligible.

INTRODUCTION

The flow phenomenon encountered by vehicles in the reentry Mach number range is very complex. The extreme heating, loading, and stability problems which the designer must cope with are in many cases incompletely understood. In the preliminary evaluation of the design of a reentry vehicle, the ability to predict pressure distributions is of fundamental importance in understanding all these aspects of the reentry problem. Thus, the present paper is concerned with assessing the adequacy of currently available methods of predicting pressures on blunt noses and in the induced-pressure region behind blunt noses on the simple axisymmetric and two-dimensional types of configurations which will form components of complete reentry vehicles. Most of the experimental work has been performed in a perfect fluid in order to simplify the understanding of the basic fluid dynamics of high Mach number flight.

SYMBOLS

b	surface distance from nose stagnation point to nose-cylinder juncture
c	chord length
$C_{D,n}$	nose drag coefficient
$C_{m,le}$	pitching moment about leading edge
C_N	normal-force coefficient
d	maximum body diameter
M_∞	free-stream Mach number
$M_{\infty,n}$	free-stream Mach number at nose
$M' = \frac{dM_\infty}{d(x/t)}$	
p	static pressure
p_∞	free-stream static pressure
$p_{\infty,n}$	free-stream static pressure at nose
$p_{\infty,l}$	free-stream static pressure at orifice location in tunnel when model is absent
p_{MAX}	maximum static pressure on model
R_d	Reynolds number based on maximum body diameter
s	surface distance measured from stagnation point
t	plate thickness
x	streamwise surface distance measured from model nose-cylinder juncture

x_{cp} center-of-pressure location, measured from model nose

α angle of attack

γ ratio of specific heats

ρ_∞ free-stream density

ρ_s density behind normal shock

L-1051

DATA REDUCTION

Much of the data in the present paper was obtained in the 2-inch helium tunnel at the Langley Research Center. This tunnel utilizes a conical nozzle. The flow in conical nozzles deviates from the desired flow in that there is a longitudinal pressure and Mach number gradient, and a lateral conical flow-angularity distribution. This deviation from the desired state raises a question of interpretation of the data.

A series of characteristics calculations was therefore performed in the Langley 11-Inch Hypersonic Tunnel Section on the two-dimensional sonic-wedge—slab illustrated in figure 1 in order to obtain a first-order picture of the effects of conical flow.

The pressure distributions shown in figure 1 were obtained by using

$$M_\infty = M_{\infty,n} + M' \frac{x}{t} \tag{1}$$

where M_∞ is the free-stream Mach number, $M_{\infty,n}$ is the free-stream Mach number at the nose, and $M' = \frac{dM_\infty}{d(x/t)}$. Pressure distributions were calculated for a constant free-stream Mach number ($M' = 0$) and for conical flow with various values of M'. Figure 1 shows the results for $M' = 0$ and $M' = 0.05$ only. The pressures for $M' = 0.05$ were normalized three different ways as shown and compared with the $M' = 0$ case.

The normalizing methods are:

Method 1 utilizes $p/p_{\infty,n}$

where p is the calculated body static pressure and $p_{\infty,n}$ is the free-stream static pressure at the nose.

Method 2 utilizes $p/p_{\infty,l}$

where $p_{\infty,l}$ is the local free-stream static pressure that would exist at the point in the flow where p is calculated if the body were not present.

L
1
0
5
1

Method 3 utilizes $\dfrac{p + (p_{\infty,n} - p_{\infty,l})}{p_{\infty,n}}$

This is the so-called "buoyancy-correction" method (ref. 1) which has been used successfully at supersonic speeds to correct the pressure drag of bodies which were tested in flow with a slight longitudinal pressure gradient.

Of the three, the buoyancy-correction method most closely represents the pressure distribution that exists for uniform flow. This method has therefore been used to normalize the data obtained in conical flow. However, the data are presented as p/p_{∞}.

The adequacy of the buoyancy-correction method in radial flow decreases with increasing x/t and with increasing M'; therefore, it must be used with caution. However, for flow with Mach number gradient but zero flow angularity, the buoyancy-correction method gives good results to the highest M' investigated ($M' = 0.2$).

OUTGASSING EFFECTS

The pressure distributions to be presented were obtained by using metal tubing with short lengths of plastic tubing in the pressure-measuring circuit. The plastic tubing was used only where necessary, was kept as short as possible, and was carefully selected to insure that it had negligible porosity. The entire system of model, metal and plastic tubing, and manometer was thoroughly outgassed prior to obtaining data. These precautions were necessary because of the low pressures encountered.

Figure 2 illustrates the effect that outgassing and porosity can have on pressure measurements. The tests were performed on a hemisphere-cylinder model in the Langley 11-inch hypersonic tunnel (ref. 2). The figure presents two sets of induced-pressure-distribution measurements. Both sets were obtained on the same model with identical flow conditions in the tunnel. The higher of the two sets of data was obtained with about 3 feet of plastic tubing exposed to the atmosphere in the pressure-measuring circuit. No attempt was made to outgas the system before obtaining data. The other set of data was obtained after the plastic tubing was replaced by metal tubing (with short plastic jumpers) which was then thoroughly outgassed before data were obtained. It can be seen that the results are in error by a factor of about 2 at $x/d \approx 8$ because of outgassing and porosity effects in the plastic tubing.

L-1051

RESULTS

Blunt-Nose Pressures

It has been well established that modified Newtonian flow theory gives good predictions of the pressure distribution on blunt bodies at Mach numbers above about 3, from the stagnation point back to the region where the angle between the free-stream flow direction and the tangent to the body surface is on the order of 30° or less, depending on the Mach number, as long as the body curvature is not so large that centrifugal-force effects must be accounted for. In the region of the nose-cylinder juncture, where entropy and vorticity effects enter the picture, Newtonian theory fails. In an attempt to eliminate this deficiency, Lees suggested modifying the theory by matching the two-dimensional Prandtl-Meyer solution to the Newtonian at the point on the body where both the body pressure and the slope of the body pressure with surface distance were the same (refs. 3 and 4). In this form, the theory predicts that the shoulder pressure will be identical on different bodies which are tested at the same Mach number.

Figure 3 shows the pressure distribution on two noses with a fineness ratio of 1. The body shapes are of the form

$$x \propto r^{n} \tag{2}$$

where x and r are Cartesian coordinates, x in the streamwise direction. In the figure, the exponents for the bodies with moderate and large bluntness are $n = 2$ and $n = 6$, respectively. It is seen that both bodies do have essentially the same shoulder pressure. The forebody

pressures are predicted fairly well by the modified Newtonian-Prandtl-Meyer theory except near the shoulder, where the lower pressure downstream of the corner expansion probably alleviates the nose pressure somewhat through the boundary layer. The agreement between theory and experiment in the region of high curvature on the $n = 6$ body is noteworthy since no centrifugal-force corrections were included. The modified blast-wave theory (ref. 5) closely predicts the pressures in the initial induced-pressure region. However, the pressures for the body with the lower nose drag ($n = 2$) are seen to decrease more with surface distance than the pressure for the $n = 6$ nose, which is in accord with the blast-wave prediction to be discussed later.

It has been pointed out in the literature that the details of the flow in the nose region of blunt bodies are affected by the shape of the sonic line (see for instance, refs. 6, 7, and 8). The sonic-line shape for a given body shape depends strongly on the density ratio across the shock. Figure 4 compares the pressure distributions on a hemisphere-cylinder obtained at hypersonic speeds by using test mediums with different density ratios across the shock. The circles represent data obtained in helium at $M_\infty = 19$ and $\rho_s/\rho_\infty \approx 4$, while the hatched areas represent data obtained in dissociated air in the AEDC Hotshot I tunnel (ref. 9) at $M_\infty = 15.6$ and $\rho_s/\rho_\infty \approx 10$. The type of sonic-line shape generated by these two flows is as illustrated. An examination of the data reveals that any differences which may exist are certainly small, even in the neighborhood of the sonic point on the body $\left(p/p_{MAX} \approx 0.5\right)$. Thus, the effect of sonic-line shape as well as effective specific-heat ratio is seen to be unimportant as far as blunt-nose-forebody pressure-ratio distributions are concerned, at least for the hemisphere nose. The theory in figure 4 is again modified Newtonian-Prandtl-Meyer and modified blast-wave.

The experimental shoulder pressure obtained in helium is seen to be higher than the theory, whereas the shoulder pressure on the models shown in figure 3 was well predicted by the theory. The value of R_d was the same for both sets of helium data. The difference in results can possibly be attributed to a shape effect; that is, the hemisphere has continuous curvature while the n-powered bodies have a finite expansion at the shoulder.

The pressure at the nose-cylinder juncture of blunt-nosed bodies is affected by a variation of Reynolds number as well as geometry; this is illustrated in figure 5 for the hemisphere-cylinder. (See ref. 2.) The figure shows the variation of p/p_{MAX} with R_d for various values of x/d. Clearly, the effects of Reynolds number can be appreciable at and close to the shoulder. The point labeled "theory" at $R_d = \infty$ is the

inviscid modified Newtonian-Prandtl-Meyer value. Except possibly at very low Reynolds numbers, the effects of Reynolds number become negligible beyond $x/d = 0.5$. This does not imply that there are no boundary-layer effects farther downstream; rather the boundary-layer effects that do exist are essentially unaffected by a variation in Reynolds number beyond $x/d = 0.5$.

It is of interest to note that the experimental points are a composite of results from the 2-inch helium tunnel and the 11-inch constant Mach number helium tunnel.

L-1051

Induced Pressures

The blast-wave analogy (see refs. 3 and 10 to 13, for example) furnishes the designer with a rapid means of estimating blunt-nose induced body pressures. However, its adequacy from the standpoint of accuracy has been seriously questioned. (See, for instance, ref. 14.) This section of the paper is devoted to assessing the usefulness of the blast-wave theory.

Figure 6 presents the results of a series of exact characteristics calculations which were made to determine the inviscid induced pressures on cylinders behind various nose shapes at Mach numbers from 6.9 to 40 in both air and helium. The calculated values have been plotted by using the blast-wave parameter and it is seen that all the results fall within a narrow band (except values closer than about 2 to 4 diameters behind the shoulder, which have been neglected). Thus, within the range of variables covered, the blast-wave theory furnishes a triple correlation parameter; that is, all the calculated pressures beyond a few body diameters from the shoulder fall within a narrow band for a wide range of Mach numbers and nose-drag coefficients, and for two values of specific-heat ratio. These theoretical results indicate that the blast-wave theory furnishes an excellent correlating parameter whose usefulness extends over a much wider range of nose drags than the assumptions upon which blast-wave theory are based would appear to warrant. Also, inherent in the nose-drag dependence is the implication that induced pressures are independent of nose shape. Thus, the models shown in figure 7 were designed to check experimentally the range of validity of the nose-shape-independence concept, and to check the extent to which induced pressures could be correlated by nose drag. There were six pairs of models. Each pair consists of two cylindrical rods with different nose shapes but the same nose drag. The nose-drag coefficients vary from 0.2 to 1.2. Pressures were obtained at x/d locations from 0.02 to 20 at $M_\infty = 21$ in helium. Figure 8 presents the results for the $C_{D,n} = 0.2$ and 1.2 bodies; these are typical of all the results.

It can be seen that except at $x/d = 0.02$, the induced-pressure distribution is essentially independent of nose shape, at least for $0.2 \leqq C_{D,n} \leqq 1.2$.

Figure 9 presents all the pressure data obtained on the models of figure 7 plotted against the blast-wave parameter $\frac{x/d}{M_\infty{}^2\sqrt{C_{D,n}}}$. As indicated in the figure, good correlation is obtained for x/d equal to or greater than 2.5.

L 1 0 5 1

Although blast-wave theory correlates induced pressures well and predicts the induced-pressure dependence on nose drag and independence of nose shape, the blast-wave theory is not capable of predicting absolute induced-pressure values, as illustrated in figure 10 for a hemisphere-cylinder (ref. 2). Because of the assumptions upon which the theory is based, the theory cannot give good results near the shoulder nor far downstream. However, blast-wave theory can be modified so that the end-point conditions (that is, the pressure at the shoulder and the pressure at an infinite distance downstream) are taken into account (ref. 5). If the Newtonian-Prandtl-Meyer prediction is used for the shoulder pressure and the value obtained from characteristics calculations is used for the far downstream pressure, the resulting modified blast-wave theory gives the lower curve in figure 10. This curve gives a good prediction of trend but is clearly too low. It should be borne in mind, however, that the end points by which the theory was modified were obtained from inviscid predictions.

It has been demonstrated earlier in the paper that the shoulder pressure varies with geometry and Reynolds number. If viscous and geometry effects are included by using the experimentally determined end points to modify the blast-wave theory, the short dashed line is obtained; it is seen to fit the measured pressure distribution. Thus, blast-wave theory can apparently be modified to predict accurately the induced-pressure distributions if some means can be found to determine the shoulder pressure and the asymptotic downstream pressure for any combination of geometry and Reynolds number. At present, no such method exists; work in this area is needed. Until a satisfactory method of modifying blast-wave theory can be found, empirical equations can be determined from the correlation plots. When x/d is measured from the shoulder, as in this paper, the correlation plots yield equations which do not apply near the shoulder. Better correlation can be obtained near the shoulder if x/d is measured from the nose; however, the correlation far downstream then becomes less satisfactory.

Two-Dimensional Induced-Pressure Effects

The large induced pressures that can occur at reentry Mach numbers may have considerable effect upon the stability of a vehicle. The magnitude of these effects and the conditions under which they may or may not be important are illustrated in figures 11 and 12. The normal-force coefficient, pitching-moment coefficient about the leading edge, and center-of-pressure location are plotted against chord-thickness ratio for a flat slab with a blunt leading edge at 5° to 20° angle of attack at $M_\infty = 20$ in perfect air.

L
1
0
5
1

The nose shape was varied with α so that both wedges had sonic velocity and the apex of the wedges lay on the center line of the slab. Although this is not a realistic configuration, it allowed the pressure distributions (which were integrated to obtain C_N and $C_{m,le}$) from reference 13 to be used. These pressure distributions were obtained by the method of characteristics and include the inviscid induced-pressure effects. The values of C_N, $C_{m,le}$, and x_{cp}/c which were derived by using these pressure distributions are compared with values of the same parameters derived by using pressure distributions determined from the tangent-wedge approximation. Of importance is the difference between these two sets of curves. It is seen that induced-pressure effects on all three parameters investigated can be large in the low angle-of-attack range. However, at 20° the contribution of the induced effects is negligible.

CONCLUDING REMARKS

The designer has adequate means at his disposal for calculating the inviscid direct and induced pressures on simple axisymmetric bodies at zero angle of attack. Viscous effects can modify these results however, particularly near the shoulder on noses and in the induced-pressure region. Additional research is needed to determine the magnitude of viscous effects for any combination of geometry and Reynolds number. Until a satisfactory means of predicting viscous effects is found, empirical equations based on the blast-wave correlating parameter can be used in the induced-pressure region.

Langley Research Center,
National Aeronautics and Space Administration,
Langley Field, Va., April 11, 1960.

REFERENCES

1. Love, Eugene S., Coletti, Donald E., and Bromm, August F., Jr.: Investigation of the Variation With Reynolds Number of the Base, Wave, and Skin-Friction Drag of a Parabolic Body of Revolution (NACA RM-10) at Mach Numbers of 1.62, 1.93, and 2.41 in the Langley 9-Inch Supersonic Tunnel. NACA RM L52H21, 1952.

2. Mueller, James N., Close, William H., and Henderson, Arthur, Jr.: An Investigation of Induced-Pressure Phenomena on Axially Symmetric, Flow-Alined, Cylindrical Models Equipped With Different Nose Shapes at Free-Stream Mach Numbers From 15.6 to 21 in Helium. NASA TN D-373, 1960.

3. Lees, Lester, and Kubota, Toshi: Inviscid Hypersonic Flow Over Blunt-Nosed Slender Bodies. Jour. Aero. Sci., vol. 24, no. 3, Mar. 1957, pp. 195-202.

4. Wagner, Richard D., Jr.: Some Aspects of the Modified Newtonian and Prandtl-Meyer-Expansion Method for Axisymmetric Blunt Bodies at Zero Angle of Attack. Jour. Aero/Space Sci. (Readers' Forum), vol. 26, no. 12, Dec. 1959, pp. 851-852.

5. Love, E. S.: Prediction of Inviscid Induced Pressures From Round Leading Edge Blunting at Hypersonic Speeds. ARS Jour. (Tech. Notes), vol. 29, no. 10, pt. 1, Oct. 1959, pp. 792-794.

6. Hayes, Wallace D., and Probstein, Ronald F.: Hypersonic Flow Theory. Academic Press, Inc. (New York), 1959.

7. Traugott, Stephen C.: Shock Generated Vorticity and Sonic Line Slope on the Surface of Blunt Bodies in Supersonic and Hypersonic Flight. RR-14, The Martin Co., Feb. 1959.

8. Van Dyke, Milton D., and Gordon, Helen D.: Supersonic Flow Past a Family of Blunt Axisymmetric Bodies. NASA TR R-1, 1959.

9. Boison, J. Christopher: Experimental Investigation of the Hemisphere-Cylinder at Hypervelocities in Air. AEDC-TR-58-20, ASTIA Doc. No.: AD-204392, Arnold Eng. Dev. Center, Nov. 1958.

10. Cheng, H. K., and Pallone, A. J.: Inviscid Leading-Edge Effect in Hypersonic Flow. Jour. Aero. Sci. (Readers' Forum), vol. 23, no. 7, July 1956, pp. 700-702.

11. Bertram, M. H., and Baradell, D. L.: A Note on the Sonic-Wedge Leading-Edge Approximation in Hypersonic Flow. Jour. Aero. Sci. (Readers' Forum), vol. 24, no. 8, Aug. 1957, pp. 627-629.

12. Henderson, Arthur, Jr., and Johnston, Patrick J.: Fluid-Dynamic Properties of Some Simple Sharp- and Blunt-Nosed Shapes at Mach Numbers from 16 to 24 in Helium Flow. NASA MEMO 5-8-59L, 1959.

13. Bertram, Mitchel H., and Henderson, Arthur, Jr.: Effects of Boundary-Layer Displacement and Leading-Edge Bluntness on Pressure Distribution, Skin Friction, and Heat Transfer of Bodies at Hypersonic Speeds. NACA TN 4301, 1958.

14. Bogdonoff, Seymour M., and Vas, Irwin E.: A Study of Hypersonic Wings and Controls. Paper No. 59-112, Inst. Aero. Sci., June 16-19, 1959.

L
1
0
5
1

DATA-REDUCTION METHODS ON A BLUNTED TWO-DIMENSIONAL FLAT PLATE IN CONICAL FLOW

$M_{\infty,n}=20$; $M'=0.05$; $\gamma=5/3$

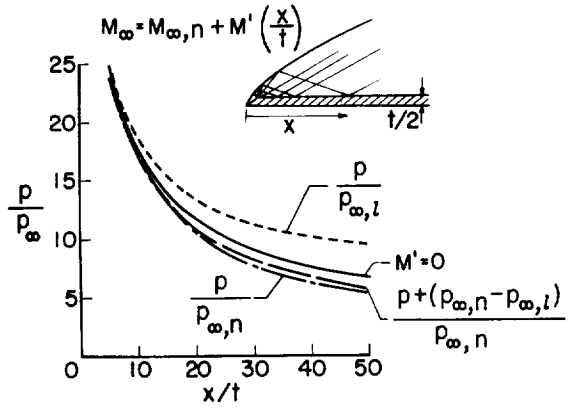

Figure 1

EFFECT OF TUBING ON HEMISPHERE-CYLINDER INDUCED PRESSURE MEASUREMENT

$M = 16.6$; $\gamma = 5/3$

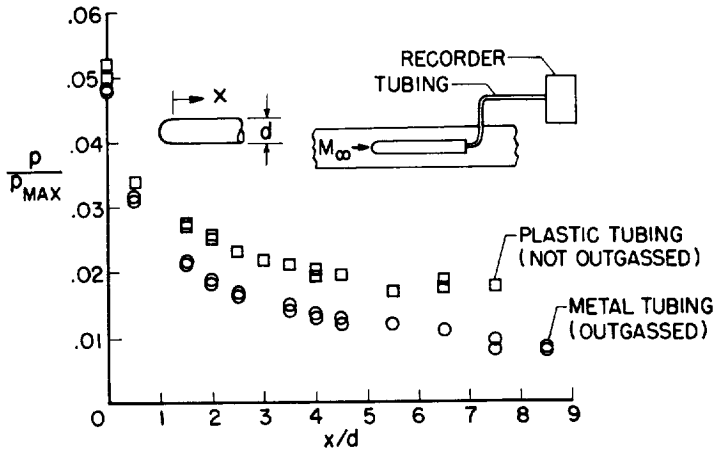

Figure 2

L-1051

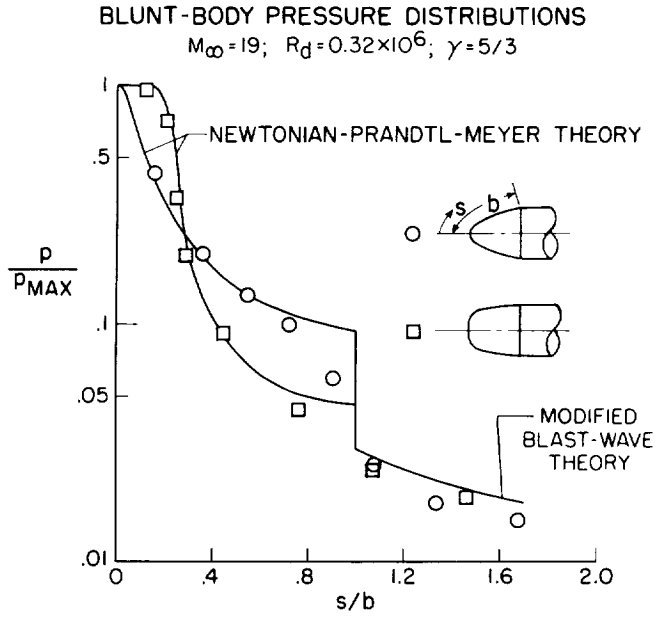

Figure 3

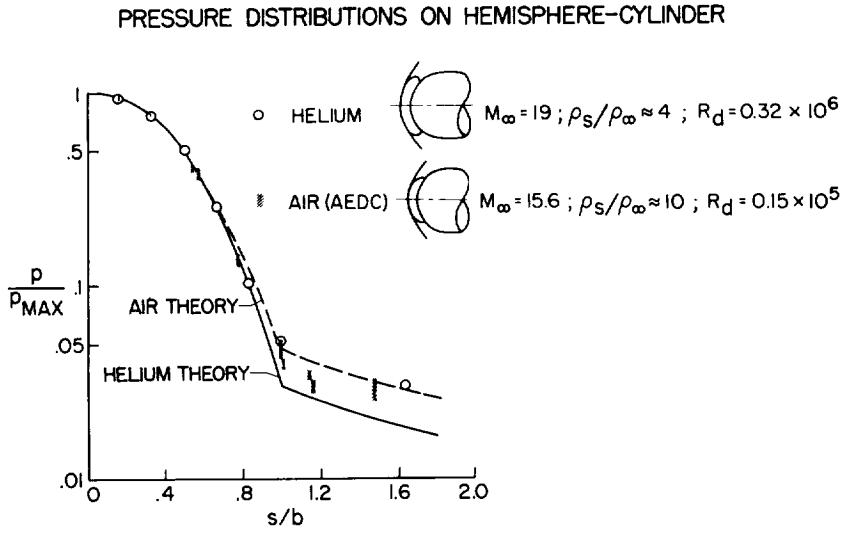

Figure 4

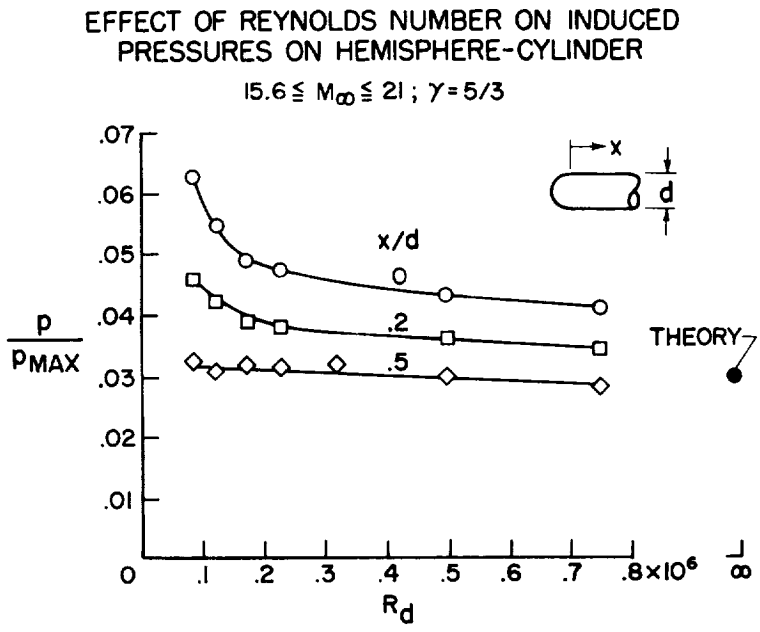

Figure 5

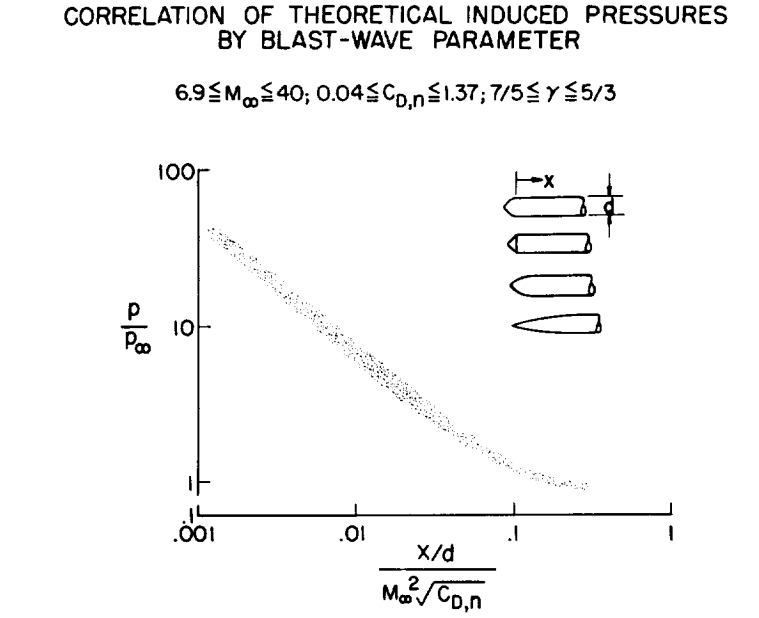

Figure 6

MODELS USED IN INVESTIGATION OF
NOSE-SHAPE-INDEPENDENCE CONCEPT

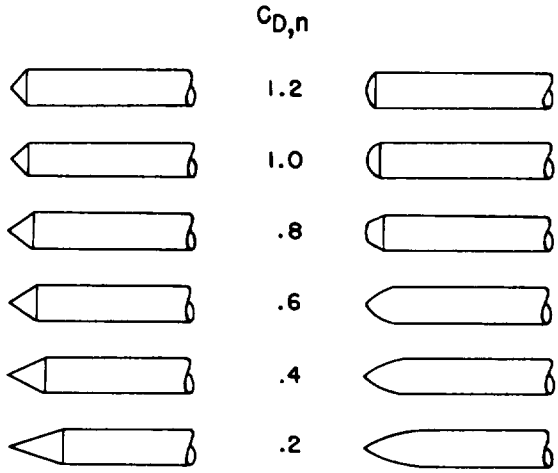

Figure 7

INDUCED PRESSURES, NOSE-SHAPE-INDEPENDENCE CONCEPT
$M_\infty = 21$, $\gamma = 5/3$

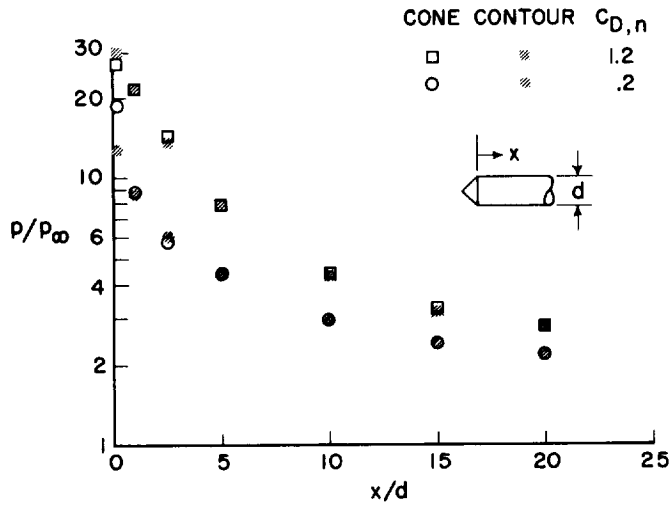

Figure 8

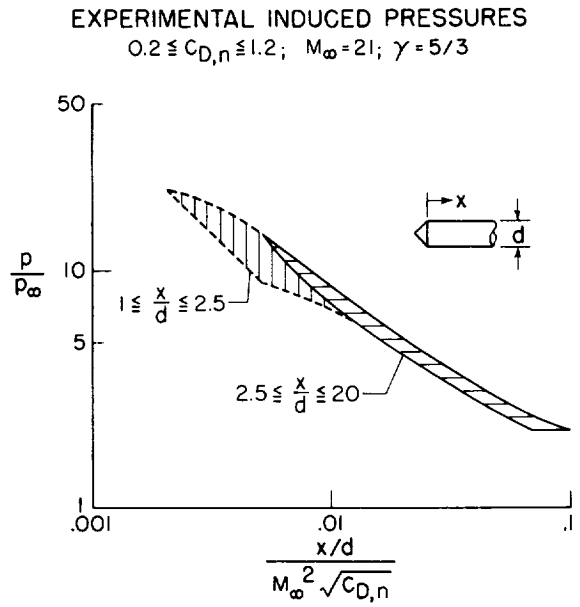

Figure 9

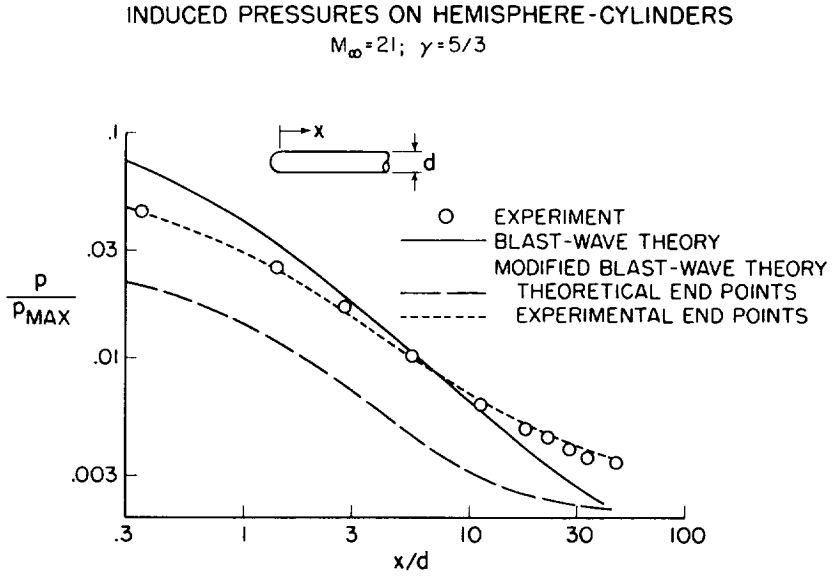

Figure 10

L-1051

EFFECT OF INDUCED PRESSURE ON TWO-DIMENSIONAL FORCE AND MOMENT CHARACTERISTICS

$M_\infty = 20$; $\gamma = 7/5$

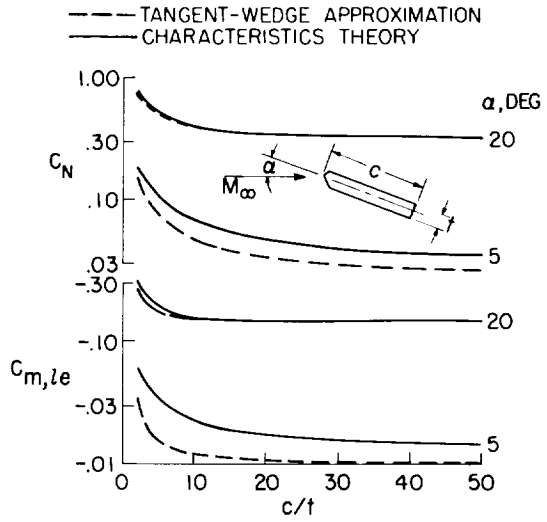

Figure 11

EFFECT OF INDUCED PRESSURE ON TWO-DIMENSIONAL CENTER-OF-PRESSURE LOCATION

$M_\infty = 20$, $\gamma = 7/5$

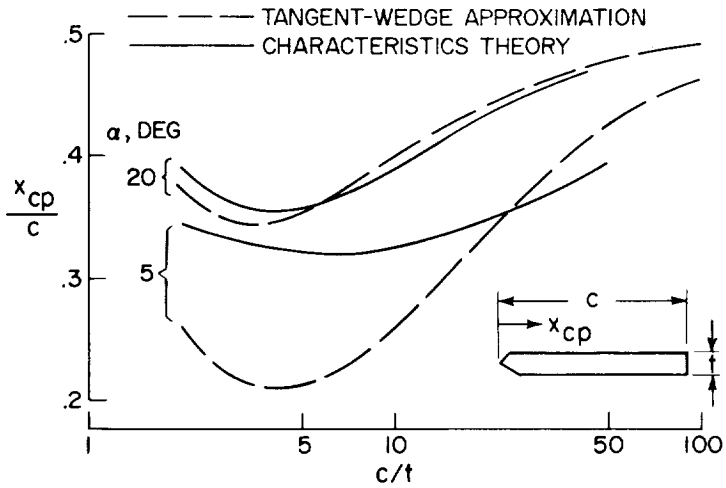

Figure 12

L-1051

NASA TN D-449
National Aeronautics and Space Administration.
INVESTIGATION OF THE FLOW OVER SIMPLE BODIES AT MACH NUMBERS OF THE ORDER OF 20.
Arthur Henderson, Jr. August 1960. 17p. OTS price $0.50. (NASA TECHNICAL NOTE D-449)

It is shown that adequate means are available for calculating inviscid direct and induced pressures on simple axisymmetric bodies at zero angle of attack. The extent to which viscous effects can alter these predictions is indicated. It is also shown that inviscid induced pressure can significantly affect the stability of blunt, two-dimensional flat wings at low angles of attack. However, at high angles of attack, the inviscid induced pressure effects are negligible.

(Initial NASA distribution: 1, Aerodynamics, aircraft; 2, Aerodynamics, missiles and space vehicles; 20, Fluid mechanics.)

I. Henderson, Arthur, Jr.
II. NASA TN D-449

NASA

NASA TN D-449
National Aeronautics and Space Administration.
INVESTIGATION OF THE FLOW OVER SIMPLE BODIES AT MACH NUMBERS OF THE ORDER OF 20.
Arthur Henderson, Jr. August 1960. 17p. OTS price $0.50. (NASA TECHNICAL NOTE D-449)

It is shown that adequate means are available for calculating inviscid direct and induced pressures on simple axisymmetric bodies at zero angle of attack. The extent to which viscous effects can alter these predictions is indicated. It is also shown that inviscid induced pressure can significantly affect the stability of blunt, two-dimensional flat wings at low angles of attack. However, at high angles of attack, the inviscid induced pressure effects are negligible.

(Initial NASA distribution: 1, Aerodynamics, aircraft; 2, Aerodynamics, missiles and space vehicles; 20, Fluid mechanics.)

I. Henderson, Arthur, Jr.
II. NASA TN D-449

NASA

NASA TN D-449
National Aeronautics and Space Administration.
INVESTIGATION OF THE FLOW OVER SIMPLE BODIES AT MACH NUMBERS OF THE ORDER OF 20.
Arthur Henderson, Jr. August 1960. 17p. OTS price $0.50. (NASA TECHNICAL NOTE D-449)

It is shown that adequate means are available for calculating inviscid direct and induced pressures on simple axisymmetric bodies at zero angle of attack. The extent to which viscous effects can alter these predictions is indicated. It is also shown that inviscid induced pressure can significantly affect the stability of blunt, two-dimensional flat wings at low angles of attack. However, at high angles of attack, the inviscid induced pressure effects are negligible.

(Initial NASA distribution: 1, Aerodynamics, aircraft; 2, Aerodynamics, missiles and space vehicles; 20, Fluid mechanics.)

I. Henderson, Arthur, Jr.
II. NASA TN D-449

NASA

NASA TN D-449
National Aeronautics and Space Administration.
INVESTIGATION OF THE FLOW OVER SIMPLE BODIES AT MACH NUMBERS OF THE ORDER OF 20.
Arthur Henderson, Jr. August 1960. 17p. OTS price $0.50. (NASA TECHNICAL NOTE D-449)

It is shown that adequate means are available for calculating inviscid direct and induced pressures on simple axisymmetric bodies at zero angle of attack. The extent to which viscous effects can alter these predictions is indicated. It is also shown that inviscid induced pressure can significantly affect the stability of blunt, two-dimensional flat wings at low angles of attack. However, at high angles of attack, the inviscid induced pressure effects are negligible.

(Initial NASA distribution: 1, Aerodynamics, aircraft; 2, Aerodynamics, missiles and space vehicles; 20, Fluid mechanics.)

I. Henderson, Arthur, Jr.
II. NASA TN D-449

NASA